



Published in final edited form as:

Nat Protoc. 2020 July ; 15(7): 2186–2202. doi:10.1038/s41596-020-0327-3.

Analysis of task-based functional MRI data preprocessed with fMRIPrep

Oscar Esteban¹, Rastko Ciric¹, Karolina Finc², Ross W. Blair¹, Christopher J. Markiewicz¹, Craig A. Moodie¹, James D. Kent³, Mathias Goncalves⁴, Elizabeth DuPre⁵, Daniel E. P. Gomez⁶, Zhifang Ye⁷, Taylor Salo⁸, Romain Valabregue⁹, Inge K. Amlie¹⁰, Franziskus Liem¹¹, Nir Jacoby¹², Hrvoje Stoji¹³, Matthew Cieslak¹⁴, Sebastian Urchs⁵, Yaroslav O. Halchenko¹⁵, Satrajit S. Ghosh^{4,16}, Alejandro De La Vega¹⁷, Tal Yarkoni¹⁷, Jessey Wright¹, William H. Thompson^{1,18}, Russell A. Poldrack¹, Krzysztof J. Gorgolewski¹

¹Department of Psychology, Stanford University, Stanford, CA, USA. ²Centre for Modern Interdisciplinary Technologies, Nicolaus Copernicus University in Toruń, Toruń, Poland.

³Neuroscience Program, University of Iowa, Iowa City, IA, USA. ⁴McGovern Institute for Brain Research, MIT, Cambridge, MA, USA. ⁵Montreal Neurological Institute, McGill University, Montreal, Canada. ⁶Donders Institute for Brain, Cognition and Behaviour, Radboud University, Nijmegen, Netherlands. ⁷State Key Laboratory of Cognitive Neuroscience and Learning, Beijing Normal University, Beijing, China. ⁸Department of Psychology, Florida International University, Miami, FL, USA. ⁹CENIR, INSERM U 1127, CNRS UMR 7225, UPMC Univ Paris 06 UMR S 1127, Institut du Cerveau et de la Moelle épinière, ICM, Paris, France. ¹⁰Center for Lifespan Changes in Brain and Cognition, University of Oslo, Oslo, Norway. ¹¹URPP Dynamics of Healthy

Reprints and permissions information is available at www.nature.com/reprints.

Correspondence and requests for materials should be addressed to O.E., phd@oscaresteban.es.

Author contributions

O.E., R.A.P. and K.J.G. contributed to conceptualization, data curation and funding acquisition. O.E., R.C. and K.F. contributed to formal analysis, investigation, methodology and validation and wrote the original draft. K.F. contributed visualizations. O.E., J.W. and W.H.T. contributed to interpretation and overall framing of the protocol. R.A.P. and K.J.G. contributed to project administration, resources and supervision. All the authors have contributed software and/or documentation, read the manuscript and edited/revised the original draft and later versions.

Reporting Summary

Further information on research design is available in the Nature Research Reporting Summary linked to this article.

Data availability

This protocol uses ds000003, a dataset publicly available at <https://openneuro.org> under the terms of the CC0 license. OpenNeuro and other neuroimaging archives contain a large number of open datasets in which this protocol can be exercised and evaluated. The outcomes of preprocessing ds000003 are available using DataLad (<https://datalad.org>) under a CC0 license, with DataLad dataset locator `///labs/poldrack/ds003_fmriprep`. Results of the analysis workflow described in this protocol are also distributed under the CC0 license and can be accessed with DataLad, with DataLad dataset locator `///labs/poldrack/NP-180740`.

Code availability

fMRIPrep is open source, available at <https://github.com/poldracklab/fmriprep> under a three-clause Berkeley Software Distribution license. The code for the exemplary analysis and visualizations is available at <https://github.com/poldracklab/ds003-post-fMRIPrep-analysis> under an Apache-2.0 license.

Competing interests

The authors declare no competing interests.

Supplementary information is available for this paper at <https://doi.org/10.1038/s41596-020-0327-3>.

Peer review information *Nature Protocols* thanks Jo Etzel and Angela Laird for their contribution to the peer review of this work.

Publisher's note Springer Nature remains neutral with regard to jurisdictional claims in published maps and institutional affiliations.

Aging, University of Zurich, Zürich, Switzerland. ¹²Department of Psychology, Columbia University, New York, NY, USA. ¹³Max Planck UCL Centre for Computational Psychiatry and Ageing Research, University College London, London, UK. ¹⁴Perelman School of Medicine, University of Pennsylvania, Philadelphia, PA, USA. ¹⁵Department of Psychological and Brain Sciences, Dartmouth College, Hanover, NH, USA. ¹⁶Department of Otolaryngology, Harvard Medical School, Boston, MA, USA. ¹⁷Department of Psychology, University of Texas at Austin, Austin, TX, USA. ¹⁸Department of Clinical Neuroscience, Karolinska Institutet, Solna, Sweden.

Abstract

Functional magnetic resonance imaging (fMRI) is a standard tool to investigate the neural correlates of cognition. fMRI noninvasively measures brain activity, allowing identification of patterns evoked by tasks performed during scanning. Despite the long history of this technique, the idiosyncrasies of each dataset have led to the use of ad-hoc preprocessing protocols customized for nearly every different study. This approach is time consuming, error prone and unsuitable for combining datasets from many sources. Here we showcase fMRIPrep (<http://fmriprep.org>), a robust tool to prepare human fMRI data for statistical analysis. This software instrument addresses the reproducibility concerns of the established protocols for fMRI preprocessing. By leveraging the Brain Imaging Data Structure to standardize both the input datasets (MRI data as stored by the scanner) and the outputs (data ready for modeling and analysis), fMRIPrep is capable of preprocessing a diversity of datasets without manual intervention. In support of the growing popularity of fMRIPrep, this protocol describes how to integrate the tool in a task-based fMRI investigation workflow.

Introduction

Mapping the response of the brain to cognitive, perceptual or motor manipulations is the primary goal of task-based functional MRI (fMRI) experiments¹. Such evoked neuronal activation triggers specific metabolic dynamics that are detected by fMRI as the magnetic susceptibility of blood changes with its oxygenation level. Blood-oxygen-level-dependent (BOLD) fluctuations track the hemodynamic response and thus indirectly map out the delivery of oxygen to active neuronal tissue across the brain² throughout the duration of an experiment. Since MRI does not require any ionizing radiation, fMRI is a minimally invasive functional imaging technique. Its safety and quite high resolution (in both space and time) at a systems scale have supported the rapid growth in the utilization of fMRI in cognitive neuroscience. The number of publications under the topic of ‘fmri’, as indexed by the Web of Science, has consistently increased from five records in 1992 to nearly 6,000 scientific articles in 2018. This body of literature covers a wide range of applications investigating the functional organization and physiology of the human and nonhuman brain, often in differential analyses with clinical populations.

However, with the sole exception of presurgical planning, fMRI is not a standard technique for clinical application. In contrast to other MRI techniques more frequently used in the clinic, fMRI is nearly impossible to interpret directly by eye. fMRI requires sophisticated

processing and statistical analyses that are robust enough to reliably disentangle the different factors contributing to the BOLD signal and select just those with neural origins that were elicited by the phenomena under study.

Platforms for collecting and sharing neuroimaging datasets, such as OpenfMRI³ and its successor OpenNeuro⁴, are quickly growing in size and reflect the increasing popularity of fMRI among researchers. The deluge of data acquired has stimulated the development of new fMRI data processing protocols. While the multiplicity of protocols has enlarged the capacity for scientific discovery, it has also worsened problems arising from the methodological variability of fMRI data analysis. For example, Carp⁵ analyzed the multiplicity of analysis workflows and called attention to the great flexibility researchers had in making choices about data processing workflows. Carp showed that increases in analytic flexibility might substantially elevate the rate of false-positive findings in the literature. More recently, Bowring et al.⁶ quantified the differences between analysis alternatives by attempting to replicate three original task-fMRI studies using different processing and analysis pipelines. To replicate three published studies with varying processing tools, the authors created three different pipelines per study, each pipeline based on a different neuroimaging toolbox. Study-wise, the authors obtained qualitatively similar results across the three pipelines corresponding with each original paper. However, they could not quantitatively replicate the original studies even with the pipeline and tool combination that matched each original paper. Thus, while researchers may report new results, it is difficult or even impossible to disentangle whether these results are the effect of the study design or the data-processing choices. Standardizing preprocessing across studies will eliminate between-study differences caused by data-preprocessing choices. This protocol addresses such concerns with fMRIPrep⁷, a standardized preprocessing pipeline for resting-state and task-based fMRI.

Development of the protocol

This protocol describes a task-based fMRI workflow that uses fMRIPrep⁷ (RRID: SCR_016216) to prepare data for statistical analysis. In this protocol, we illustrate the use of fMRIPrep on a publicly available dataset (ds000003⁸, accessible at <http://openneuro.org>). We illustrate first-level and second-level statistical analyses carried out with a minimalistic Nipype⁹ workflow composed of widely used FSL¹⁰ tools. The section ‘How to report results obtained using this protocol’ in Anticipated results details the implementation of the protocol to analyze the example dataset. Before preprocessing, the protocol includes a stage that quality-assesses the original data with MRIQC¹¹ (<https://mriqc.rea.dthedocs.io>). An overview of the workflow is given in Fig. 1.

As further described in our primary research paper first using this protocol⁷, fMRIPrep leverages the Brain Imaging Data Structure¹² (BIDS) to understand all the particular features and available metadata (i.e., imaging parameters) of the input dataset (Box 1). BIDS allows fMRIPrep to automatically configure an appropriate preprocessing workflow without manual intervention. To do so, fMRIPrep self-adapts to the dataset by applying a set of heuristics that account for irregularities such as missing acquisitions or runs. Adaptiveness is implemented with modularity: fMRIPrep is composed of sub-workflows, which are

dynamically assembled into appropriate configurations. These building blocks combine tools from widely used, open-source neuroimaging packages. The workflow engine Nipype is used to stage the workflows and deal with execution details (such as resource management).

Applications of the protocol

fMRIPrep is agnostic with respect to currently available analysis designs: it supports a range of subsequent analysis and modeling options. The range of possible applications includes within-subject analysis using functional localizers, voxel-based analysis, surface-based analysis, task-based group analysis, resting-state connectivity analysis and others. fMRIPrep outputs the preprocessed data following the BIDS-Derivatives specification¹³, which defines a consistent organizational scheme for the results of neuroimage processing. The regularity imposed by BIDS-Derivatives maximizes data compatibility with subsequent analysis and is demonstrated here with an example of a first- and second-level analysis workflow.

Limitations

Several types of fMRI data cannot be processed by this protocol, and there are other considerations that must be borne in mind (such as limitations of fMRIPrep precluding the execution on particular datasets).

High-performance computing (HPC) and Singularity—This protocol assumes that execution takes place on an HPC cluster and that both the simple Linux utility for resource management (SLURM) scheduler and the Singularity container framework are installed. However, we understand that execution on more flexible systems (e.g., commercial cloud or personal computer (PC)) should be easier than HPC systems.

Other fMRI techniques—fMRIPrep does not preprocess non-BOLD fMRI data. Of note, the current BIDS specification does not support these data types.

Animal species—fMRIPrep currently does not support nonhuman species, although we are currently exploring the processing of nonhuman primate and rodent BOLD fMRI.

Quality control of MRI data—Here, we propose MRIQC for the assessment of the acquired (unprocessed) data. We also recommend specifying clear exclusion criteria before assessment. To our knowledge, there is no consensus on a data curation protocol; laboratories currently address the problem by applying their internal know-how and subjective assessments, or by skipping the data-curation step altogether. An ultimate curation protocol remains the subject of active discussion in the field. Describing such a protocol to check the quality of unprocessed data is beyond the scope of this article.

fMRIPrep does not run any analysis or preprocessing tailored to specific analyses—However, the BIDS-Derivatives specification allows users to connect spatio-temporal filtering tools before analysis flexibly (e.g., the XCP Pipeline¹⁴ for functional connectivity analysis, or fMRIDe-noise¹⁵ for a more general-purpose option).

Other limitations—Data from individuals presenting gross structural abnormality must be used with extreme caution, as their spatial normalization might not be optimal. Acquisitions with a very narrow field of view (e.g., focusing on the visual cortex only) may be used with caution, as intra-subject co-registration to the anatomical reference will be challenging.

Alternative fMRI protocols

Other fMRI techniques—Although fMRIPrep focuses on the preprocessing of BOLD fMRI, other MR imaging sequences exist to measure functional activity via mechanisms other than BOLD. Examples of non-BOLD contrasts used for fMRI include: (i) cerebral blood flow, commonly measured with arterial spin labeling techniques¹⁶; (ii) cerebral blood volume, measured either with iron-oxide contrast agents¹⁷ or with the non-invasive vascular space occupancy¹⁸ technique; and (iii) cerebral metabolic rate of oxygen, measured with calibrated BOLD acquisitions where subjects undergo CO₂ or O₂ gas breathing challenges¹⁹. The application, standardization and availability of non-BOLD alternatives are still marginal, as compared to BOLD, because of their more limited sensitivity. fMRIPrep could potentially cover non-BOLD fMRI with substantial adaptations (e.g., intensity distribution enhancements to counteract lower signal-to-noise ratios), once these techniques become standard.

Animal fMRI—Although fMRIPrep permits the replacement of the default MRI templates with custom alternatives, this protocol does not support animal fMRI. We are actively working on extensions to fMRIPrep for processing rodent and nonhuman primate fMRI. Most of the adaptations required for the primate fMRI extension relate to average MRI templates and pattern recognition techniques based on them. Conversely, the rodent fMRI extension requires more fundamental changes beyond the addition of appropriate MRI templates, as the MR protocol is largely different from that typically prescribed for humans and nonhuman primates.

Alternative pipelines for the preprocessing of BOLD fMRI—Depending on the particular characteristics of each study, researchers might find alternative protocols better adapted to their needs. For instance, the Configurable Pipeline for the Analysis of Connectomes²⁰ is an appropriate solution for researchers in need of a highly configurable tool to run connectivity analysis of resting-state fMRI. Similarly, when the research questions and the acquisition protocol, device and settings closely follow the imaging prescriptions from the Human Connectome Project (HCP²¹), the HCP Pipelines²² might be better suited. Table 1 summarizes some existing alternatives to fMRIPrep, describing some relative advantages and limitations of each approach.

Experimental design—BOLD fMRI is not a quantitative imaging modality. Accordingly, the experiment must be carefully designed to discriminate relative changes in the BOLD signal with respect to a reference or baseline. The experimental design is intimately related to (and largely determines aspects of) an overall statistical model that will be applied. Traditionally, such a statistical model is decoupled in two analysis levels: (i) a task model specification at the participant level (often referred to as ‘first level’) incorporating information about conditions and artifactual signals and specification of contrasts of interest

between conditions and/or their transformations, and (ii) a group level ('second level') model to draw population inferences on contrasts of interest from the participant level. For an introduction to fMRI experimental design, refer to Poldrack et al.²³. The BIDS specification includes a prescription for encoding the task paradigm in the raw dataset (files terminated with `_events.tsv`, Box 1), and fMRIPrep generates preprocessed BOLD images ready for analysis and time series corresponding to nuisance regressors (see Anticipated results for specific naming conventions). The task paradigm and preprocessed data can then be used as inputs to standard software libraries for statistical analysis of functional images. Alongside the inputs provided by fMRIPrep, these software libraries typically require additional specifications of activation contrasts, nuisance regression models and additional parameters for statistical analysis workflows. A comprehensive guide to using the nuisance regressors and general discussions about fMRI signal regression are now available within the documentation site. For more advanced topics on design efficiency, sample sizes and statistical power, multiple comparisons, etc., refer to the work by Durnez et al. (www.neuropowertools.org) and Mumford and Nichols^{24,25}.

Materials

Subject data

In this protocol, we use ds000003, an open dataset accessed through <https://openneuro.org> as an example dataset. The dataset was collected as part of Xue et al.⁸ and contains a rhyme verification task where subjects were presented with pairs of either words or pseudowords and made rhyming judgments for each pair **▲ CRITICAL** Data acquired and/or used in the study must have been acquired after approval by the appropriate ethical review board. Informed consent must have been obtained from participants. If the data are intended to be shared in a public repository such as OpenNeuro (which is recommended), the consent form submitted to the ethical review board should explicitly state that data will be publicly shared (e.g., the Open Brain consents²⁶), and, if appropriate, the consent form and the data management plan must also comply with any relevant privacy laws regarding pseudo-anonymization (e.g., General Data Protection Regulation in the European Union and the Health Insurance Portability and Accountability Act in the United States) **▲ CRITICAL** All subjects' data must be organized according to the (BIDS¹² specification. We recommend that the dataset be validated using the BIDS Validator. Conversion to BIDS and the validation with BIDS Validator are further described below.

Equipment setup

MRI scanner—If the study is acquiring new data, then a whole-head, BOLD-capable scanner is required. fMRIPrep has been tested on images acquired at 1–3 Tesla field strength. Recent multi-band echo-planar imaging sequences are supported, although all performance estimates given in this document derive from benchmarks on single-band datasets. fMRIPrep autonomously adapts the preprocessing workflow to the input data, affording researchers the possibility to fine-tune their MR protocols to their experimental needs and design.

Computing hardware—fMRIPrep is amenable to execution on almost any platform with enough memory: PC, HPC or cloud. Some elements of the workflow will require a minimum of 8 GB RAM, although 32 GB is recommended. fMRIPrep is able to optimize the workflow execution via parallelization. The use of 8–16 CPUs is recommended for optimal performance. To store interim results, fMRIPrep requires ~450 MB of hard-disk space for the anatomical workflow and ~500 MB for each functional BOLD run per subject. Therefore, a dataset with an imaging matrix of $90 \times 90 \times 70$ voxels and a total of 2,500 timepoints across all its BOLD runs will typically require ~3 GB of temporary storage. This storage can be volatile, e.g., ‘local’ scratch in HPC, which is a fast, local hard disk installed in the compute node that gets cleared after execution.

Visualization hardware—The tools used in this protocol generate HTML reports to carry out visual quality control. These reports contain dynamic, rich visual elements to inspect the data and results from processing steps. Therefore, a high-resolution, high-static contrast and widescreen monitor (>30 inches) is recommended. Visual reports can be opened with Firefox or Chrome browsers, and graphics acceleration support is recommended.

Computing software—fMRIPrep can be manually installed (‘bare-metal’ installation as per its documentation) on Linux and OSX systems or executed via containers (e.g., using Docker for Windows). When setting up manually, all software dependencies must also be correctly installed (e.g., Analysis of Functional NeuroImages (AFNI)²⁷, Advanced Normalization Tools (ANTs)²⁸, the FMRIB Software Library (FSL)¹⁰, FreeSurfer²⁹, Nilearn³⁰ and Nipype⁹). When using containers (which is recommended), a new Docker image is provided from the Docker Hub for each new release of fMRIPrep, and it includes all the dependencies pinned to specific versions to ensure the reproducibility of the computational framework. Containers encapsulate all necessary software required to run a particular data-processing pipeline akin to virtual machines. However, containers leverage some lightweight virtualization features of the Linux kernel without incurring much of the performance penalties of hardware-level virtualization. For these two reasons (ease and reproducibility), container execution is preferred. This protocol recommends running quality control on the original data before preprocessing, using MRIQC. MRIQC is a companion tool to fMRIPrep to perform a quality assessment of the anatomical and functional MRI scans, which account for the most relevant data within the typical fMRI protocol. The tool is distributed as a Docker image (recommended) and as a Python package.

Procedure

Preliminary work: acquisition and/or formatting inputs

1. Acquire new (option A) or existing (option B) dataset.
 - A. Option A: acquiring a new dataset ● **Timing** 15 min for each subject’s preparation, 30–60 min for acquisition from each subject and 15 min + 2 min per subject for organization into the BIDS format
 - i. *Participant preparation.* Obtain informed consent from subjects, collect prescribed phenotypic information (e.g., sex,

handedness, etc.), and prepare the participant for the scanning session.

- ii. *MRI acquisition.* Run the prescribed protocol, including at least one high-resolution (1 mm³, isotropic) T1-weighted (T1w) image for anatomical reference. Including a B0 field-mapping scheme supported by fMRIPrep within the acquisition protocol is an important design consideration (and recommended) to better account for geometrical distortions introduced by field inhomogeneities typically present in echo-planar imaging schemes employed in BOLD acquisitions. To afford higher accuracy in surface-based analyses, we recommend including one or more anatomical T2-weighted images within the protocol. Acquisition of simultaneous multi-slice—or ‘multiband’—sequences frequently yields functional images with lower tissue contrast than that of single-band sequence acquisitions. Therefore, we recommend adding at least one single-band reference acquisition in the protocol to supplement multiband sequences. Single-band acquisitions can improve the results of image-processing routines like boundary-based co-registration, which are guided by the contrast gradients between tissues.

▲ **CRITICAL STEP** Storing the data in DICOM (Digital Imaging and Communications in Medicine) format is critical to keep a pristine copy of the original metadata. We recommend the naming conventions of ReproIn³¹ for all sequences in the protocol to ease the following conversion step.

- iii. *DICOM to BIDS conversion.* Store all imaging data in NIfTI-1 or NIfTI-2 file formats as per BIDS specifications (Box 1), ensuring that all metadata are correctly encoded. The process can be made much more reliable and consistent with conversion tools such as HeuDiConv³². ReproIn automates the conversion to BIDS with HeuDiConv, ensuring the shareability and version control of the data starting from the earliest steps of the pipeline.

▲ **CRITICAL STEP** If data are to be shared publicly, and depending on the applicable regulations, they must be anonymized, and facial features may need to be removed from the anatomical images (some tools and recommendations are found with the Open Brain consent project²⁶).

- B. Option B: reusing a publicly available dataset ● **Timing** depends on the original data organization and availability of parameters

- i. Organize dataset in the BIDS format.

▲ **CRITICAL STEP** If the dataset is not originally shared in the BIDS format, it must be reorganized to conform to the BIDS specification using custom scripts. Box 2 shows an example of how to fetch a BIDS dataset from OpenNeuro.

Dataset validation ● **Timing** 1 min

1. Make sure the dataset fulfills the BIDS specifications with the BIDS Validator. To ensure that the dataset is BIDS compliant, use the online BIDS Validator at <https://bids-standard.github.io/bids-validator/> (or some up-to-date, local, native or containerized installation), specifying the path to the top-level directory of the dataset in the Choose File dialog. The online BIDS Validator can be run in any modern browser without uploading any data. After confirming that the dataset is BIDS compliant, manually examine and validate relevant, but non-mandatory, metadata fields (e.g., make sure that all field maps have set a valid IntendedFor key for susceptibility distortion correction).

? TROUBLESHOOTING

Set-up of the computing environment ● **Timing** 15 min

▲ **CRITICAL** The protocol is described assuming that execution takes place on an HPC cluster including the SLURM scheduler³³ and with the Singularity container framework³⁴ (v3.0 or higher) installed. With appropriate modifications to the batch directives, the protocol can also be deployed on HPC clusters with alternative job management systems such as SGE (Sun Grid Engine) or PBS (Portable Batch System). For execution in the cloud or on PC, please refer to the tool's documentation and the `fmripred-docker` tutorial³⁵.

1. When running fMRIPrep for the first time in a new computing environment, begin by building a container image. If using Singularity 2.5 or later, it is straightforward to do so via the Docker registry:

```
singularity build $STUDY/fmripred-1.4.1.simg docker://
poldracklab/
fmripred:1.4.1
```

2. Here and below `$STUDY` refers to the directory containing all study materials. Replace the path `$STUDY/fmripred-1.4.1.simg` with the local install location for the container image, and be sure to indicate a specific version of fMRIPrep (version 1.4.1, in this example). In addition to fMRIPrep, this protocol leverages the BIDS-Apps standard with MRIQC29 and the exemplar analysis workflow. Container images for MRIQC and the analysis workflow are built with `singularity build`, again substituting the local installation path as appropriate:

```
singularity build $STUDY/mriqc-0.15.1.simg docker://
poldracklab/mriqc:0.15.1
```

```
singularity build $STUDY/analysis-0.0.3.simg docker://
poldracklab/ds003-example:0.0.3
```

3. The location of the dataset (BIDS compliant) must also be noted. In this protocol, we use `$STUDY/ds000003/` as an example; the dataset path should be substituted as appropriate. The recommended way of executing fMRIPrep is to process one subject per container instance. Each container instance can make use of multiple CPUs to accelerate subject-level processing. Multiple container instances can be distributed across compute nodes to parallelize processing across subjects. ▲ **CRITICAL** All datasets used in any study (and all subjects in any dataset) should be processed consistently, using the same version of fMRIPrep. The version of fMRIPrep previously used to process any dataset can be identified by consulting the `PipelineDescription` field of the `dataset_description.json` file in the top level of fMRIPrep's output directory.

Running MRIQC¹¹ and inspecting the visual reports ● **Timing** 7–60 min of computing time and 5–15 min of researcher time per subject; scales with the BOLD-run count

1. Important: MRIQC is a tool to inspect the input dataset and flag subjects/sessions/runs that should be excluded from the analysis for their insufficient quality. Running MRIQC follows the same instructions given for fMRIPrep (see the following section).
2. Create a batch prescription file `$STUDY/mriqc.sbatch` (see Fig. 2 for the example with fMRIPrep).
3. Submit the job to the scheduler: `sbatch $STUDY/mriqc.sbatch`. Although the default options are probably sufficient, the documentation of MRIQC provides more specific guidelines.

? TROUBLESHOOTING

4. After running MRIQC, inspect all the generated visual reports to identify images with insufficient quality for analysis. Although there is not a consensus on the rules for exclusion, and they depend on the analyses planned, we recommend having these criteria pre-defined before quality assessment. Some examples of artifacts that could grant exclusion of images from a study are T1w images showing extreme ringing as a result of head motion, irrecoverable signal dropout derived from susceptibility distortions across regions of interest, excessive N/2 ghosting within fMRI scans, excessive signal leakage through slices in multiband fMRI reconstructions, etc. We did not exclude any image for

quality reasons before preprocessing with fMRIPrep and subsequent analysis in the exemplar analysis of data generated with this protocol. Should any image meet the exclusion criteria, stop the protocol at this step for that particular image.

Running fMRIPrep ● **Timing** 2–15 h of computing time per subject, depending on the number and resolution of BOLD runs, T1w reference quality, data acquisition parameters (e.g., longer for multiband fMRI data) and the workflow configuration

1. Run fMRIPrep. Figure 2 describes an example of batch prescription file `$STUDY/fmriprep.sbath` and the elements that may be customized for the particular execution environment: `sbath $STUDY/fmriprep.sbath`

? TROUBLESHOOTING

Inspection of all visual reports generated by fMRIPrep ● **Timing** 5–20 min per subject, depending on the number of BOLD runs

1. Alongside the corresponding preprocessed data (Box 3, Outcomes), fMRIPrep will generate one HTML (hypertext markup language) report per subject. Screen these reports to ensure sufficient quality of preprocessed data (e.g., accuracy of image registration processes, correctness of artifact correction techniques, etc.). Checking the visual reports from fMRIPrep ensures that the T1w reference brain was accurately extracted, adequate susceptibility distortion correction was correctly applied, an acceptable brain mask was calculated from the BOLD signal, the alignment of BOLD and T1w data was accurate, etc. If the report is satisfactory, proceed to the next step.

Transparent reporting with the citation boilerplate ● **Timing** 1 min

1. Make sure you acknowledge all the authors that created the original tools and reproducibly report the preprocessing using the citation boilerplate. For the example presented in this protocol, please refer to How to report results obtained using this protocol (in Anticipated Results) and Box 4.

Running first-level analysis on a preprocessed dataset ● **Timing** 5–60 min of computing time, depending on the number of BOLD runs and the workflow configuration

1. Determine an appropriate workflow and model design to be used for computing voxelwise activation contrasts. For this purpose, we provide reference Nipype workflows³⁶ that execute first- and second-level analysis on the example dataset using tools from FSL (principally FEAT, FMRIB's improved linear model (FILM), and FMRIB's local analysis of mixed effects (FLAME)). To make use of these workflows with a new dataset, the code should be modified so that the statistical

analysis is performed using the most appropriate contrasts. Create a batch prescription file `$STUDY/analysis.sbatch` akin to the script proposed in Fig. 2, replace the Singularity image with the one packing the analysis workflow³⁶ and finally submit the job to the scheduler:

```
sbatch $STUDY/analysis.sbatch.
```

Visualization of results ● **Timing** 5–20 min

1. Visualize results with Nilearn’s plotting functions. Here, we list examples of figures that can be generated, although most neuroimaging toolboxes include alternative utilities as well.
 - Select the group z-stat map thresholded to preserve the strongest activations. Use either maps thresholded for a desirable cluster size or maps corrected for family-wise error rate or false discovery rate.
 - *Glass brain visualization.* Plot thresholded z-stat maps on the glass brain using the `nilearn.plotting.plot_glass_brain` function. A glass brain plot shows all significant clusters on a single brain image. Set `display_mode` option to ‘lyrz’ to plot the brain activations from all four directions: ‘l’: left sagittal, ‘y’: coronal, ‘r’: right sagittal, ‘z’: axial.
 - *Brain section visualization.* Visualize thresholded z-stat maps of brain sections using the `nilearn.plotting.plot_stat_map` function. Set sections to ‘z’ (axial), ‘x’ (sagittal) and ‘y’ (coronal) to show activations in all three directions. Set the number of slices to visualize in each direction using the `cut_coords` parameter.
 - *3D brain surface visualization.* Create a 3D visualization on the inflated brain surface using the `nilearn.plotting.plot_surf_stat_map` function.
- ▲ **CRITICALSTEP** FSL and Nilearn implement Steps 6 and 7 of this example analysis; however, the outputs follow the BIDS-Derivatives specification to maximize the compatibility with alternative tools such as AFNI, SPM or FitLins.

Troubleshooting

From the many questions the source code repository and the <https://neurostars.org> channel receive weekly, it seems that some of the most common pitfalls encountered by fMRIPrep users relate to resource management and other set-up settings (Steps 3–5 in the Procedure). In particular, the limitations imposed by each HPC system and the particularities of the Singularity container framework generally require some troubleshooting.

Invalid BIDS dataset (Step 2)

A fairly common reason for fMRIPrep to fail is the attempt to use non-BIDS data. Therefore, the first troubleshooting step is running the BIDS Validator. When using containers, if the container does not have access to the data, the validator will flag the

dataset as invalid. Containers are a confined computation environment, and they are not allowed to access the host's filesystems, unless explicit measures are taken to grant access (i.e., mounting or binding filesystems). Therefore, when using containers with a valid BIDS dataset, the 'invalid BIDS dataset' could be a symptom of failure to access the data from the host.

FreeSurfer license file (Step 10)

FreeSurfer requires a license file to operate correctly. Users must obtain their license file at <https://surfer.nmr.mgh.harvard.edu/registration.html>. When using containers, the license file must be made available at a path accessible by the container. fMRIPrep's documentation is quite thorough on how to fix this issue.

Network file system errors (Steps 8 and 10)

fMRIPrep is built on Nipype⁹, a neuroimaging workflow framework that uses the file system to coordinate the data flow during execution. Network file systems may exhibit large latencies and temporary inconsistencies that may break execution. Setting the 'working directory' option (-w) to a local, synchronized file system will preempt these issues.

Memory errors (Steps 8 and 10)

When running on systems with restrictive memory-overcommit policies (frequently found in multi-tenant HPC systems), the fMRIPrep virtual memory footprint may become too large, and the process will be stopped by the scheduler or the kernel. The recommendation in this scenario is to split (parallelize) processing across subjects (Box 1 showcases a solution). Alternatively, when running on a system with 8 GB RAM, fMRIPrep is likely to exceed physical memory limits. This scenario is particularly common when running the container version of fMRIPrep, but the container has access to a very low physical memory allocation. For example, Docker typically limits memory to 2 GB by default on OSX and Windows systems. In this case, the only solution is to enlarge the memory allocation available to fMRIPrep (via adequate settings of the container engine and/or upgrading the hardware).

Hard-disk quotas (Steps 8 and 10)

Shared systems generally limit the hard-disk space a user can use. Please allocate enough space for both interim and final results. Remove interim results as soon as satisfied with the final results to free up scratch space.

NeuroStars forum

Many other frequently asked questions are found and responded to at <https://neurostars.org>. New support requests are welcome via this platform.

Anticipated results

Outcomes

The successful application of this protocol produces the outcomes described below.

Preprocessed task-based fMRI data—To maximize shareability and compatibility with potential downstream analyses, preprocessed data are organized following the BIDS-Derivatives convention. BIDS-Derivatives is an ongoing effort to extend to preprocessed data (derivatives) the BIDS specifications for original data¹³. Box 3 provides an example of such organization, indicating the files that were used on the analysis steps of this protocol.

Visual reports for quality assessment of preprocessing—fMRIPrep generates one visual report per subject. Use these to ensure that the preprocessed data meet your quality control standards.

Participant-level task-activation maps—Figure 3 shows the activation maps for the subject with identifier ‘10’ for the contrast task-vs.-nontask in the example OpenNeuro dataset ds000003. These maps were created with the analysis workflow, processing derivatives produced by fMRIPrep as appropriate (Box 3):

- Preprocessed BOLD runs spatially normalized to standard space:
derivatives/sub-`<subject_id>`/func/sub-`<subject_id>`_task-rhymejudgement_space-MNI152N-Lin2009cAsym_desc-preproc_bold.nii.gz.
- Brain mask corresponding to each preprocessed BOLD run, in standard space:
derivatives/sub-`<subject_id>` /func/sub-`<subject_id>`_task-rhymejudgement_space-MNI152NLin2009cAsym_desc-brain_mask.nii.gz.
- Confound signals, a file corresponding to each BOLD run: derivatives/sub-`<subject_id>`/func/sub-`<subject_id>`_task-rhymejudgement_space-MNI152NLin2009cAsym_-desc-confounds_regressors.tsv.

The exemplar analysis workflow³⁶ requires some information encoded within the original BIDS dataset:

- The original events file that describes when the subject was exposed to the experimental manipulation (being the presentation of words or pseudowords in the example at hand): ds000003/sub-`<subject_id>`/func/sub-`<subject_id>`_task-rhymejudgement_events.tsv.
- The repetition time for the BOLD acquisition, which is a mandatory metadata field of every BOLD run in the dataset.

Group-level task-activation maps—Figure 4 displays the group-level activation map resulting from group analysis.

How to report results obtained using this protocol

For each subject preprocessed with fMRIPrep, the tool generates a human-language description of all the preprocessing steps, including citations to the corresponding original

methods. Box 4 shows such a ‘citation boilerplate’, generated for the exemplary dataset in the context of this paper.

Exemplar analysis of data generated with this protocol

This final section describes the analysis framework we set up³⁶ to illustrate the applicability of the protocol. Therefore, the following methodological description is not automatically generated by fMRIPrep.

First-level analysis of the task-vs.-nontask contrast—First, the functional images were spatially smoothed with SUSAN (Smallest Univalve Segment Assimilating Nucleus)³⁷, using a Gaussian kernel (full-width at half-maximum of 6 mm) and filtered with a high-pass Gaussian filter (full-width at half-maximum cut-off period of 100 s). Second, the design matrix was constructed from the model specification. The first columns of the matrix describe the stimulus/condition vectors, whose elements represent the onsets and durations of the stimuli (box-car function) convolved with the hemodynamic response function, modeled with a double-gamma function including first and second derivatives. The number of stimulus regressors in the design matrix depends on the task and research questions. For purposes of this demonstration, we defined one task regressor (‘intask’) representing onsets and durations of the time frames when the task was present—either a word or a pseudoword was presented on the screen.

Besides the stimulus regressor, the design matrix also includes confounding regressors calculated via fMRIPrep. For this demonstration, we selected DVARS (D, temporal derivative of time courses; VARS, RMS variance over voxels), framewise displacement, six anatomical component-based noise correction (CompCor) components and four cosine drift terms. We note that it is the user’s choice which confounding regressors should be introduced in the first-level analysis. Therefore, we are not recommending this particular selection over any other possibility in this protocol.

Finally, the model was estimated with FILM³⁸, and a contrast was defined to extract the effect size map for task-vs.-nontask.

Group analysis of the task-vs.-nontask contrast—Group-level analysis was performed with FLAME³⁹ using statistical maps derived from the first-level analysis (‘task-vs.-nontask’ contrast). The generalized linear model (GLM) was fitted with ordinary least squares to perform voxel-wise one-sample *t* tests and extract the activation pattern consistent across participants. In brain activation analysis, statistical tests are performed voxelwise, and the large number of voxels inflates the risk of false positives among the voxelwise results. Accordingly, two forms of correction for multiple comparisons were performed: family-wise error correction with a two-tailed probability of 0.05 and cluster-based thresholding using a *z* threshold of ± 3.2 and a two-tailed probability threshold of 0.05. In line with previous studies, positive brain activation in response to reading words or pseudowords was observed in bilateral visual areas, the bilateral precentral gyrus, the cerebellum and the left angular gyrus^{40,41}. Negative activation was observed in regions of the brain’s default network, including the precuneus, the ventromedial frontal cortex and the temporo-parietal junction.

Supplementary Material

Refer to Web version on PubMed Central for supplementary material.

Acknowledgements

We thank the many community contributors who have helped fMRIPrep with code and documentation (github.com/poldracklab/fmriprep/blob/master/.maint/contributors.json). This work was supported by the Laura and John Arnold Foundation (R.A.P. and K.J.G.), the NIH (grant NBIB R01EB020740; S.S.G.) and NIMH (R24MH114705 and R24MH117179; R.A.P.). K.F. was supported by the Foundation for Polish Science, Poland (START 23.2018). D.E.P.G. was supported by a Marie Curie FP7-PEOPLE-2013-ITN ‘Initial Training Networks’ Action from the European Union (Project Reference Number: 608123). F.L. was supported by the University Research Priority Program ‘Dynamics of Healthy Aging’ at the University of Zurich. N.J. was supported by a National Science Foundation Graduate Research Fellowship (grant number DGE 16-44869). H.S. was supported by the Max Planck Society, Munich, Germany (grant number 647070403019). S.U. and E.D. were supported by Brain Canada.

References

1. Poldrack RA & Farah MJ Progress and challenges in probing the human brain. *Nature* 526, 371–379 (2015). [PubMed: 26469048]
2. Ogawa S, Lee TM, Kay AR & Tank DW Brain magnetic resonance imaging with contrast dependent on blood oxygenation. *Proc. Natl Acad. Sci. USA* 87, 9868–9872 (1990). [PubMed: 2124706]
3. Poldrack RA et al. Toward open sharing of task-based fMRI data: the OpenfMRI project. *Front. Neuroinformatics* 7, 12 (2013).
4. Gorgolewski KJ, Esteban O, Schaefer G, Wandell B & Poldrack RA OpenNeuro—a free online platform for sharing and analysis of neuroimaging data. in *Organization for Human Brain Mapping 1677* (2017).
5. Carp J On the plurality of (methodological) worlds: estimating the analytic flexibility of fMRI experiments. *Front. Neurosci* 6, 149 (2012). [PubMed: 23087605]
6. Bowring A, Maumet C & Nichols TE Exploring the impact of analysis software on task fMRI results. *Hum. Brain Mapp* 40, 3362–3384 (2019). [PubMed: 31050106]
7. Esteban O et al. fMRIPrep: a robust preprocessing pipeline for functional MRI. *Nat. Methods* 16, 111–116 (2019). [PubMed: 30532080]
8. Xue G & Poldrack RA The neural substrates of visual perceptual learning of words: implications for the visual word form area hypothesis. *J. Cogn. Neurosci* 19, 1643–1655 (2007). [PubMed: 18271738]
9. Gorgolewski K et al. Nipype: a flexible, lightweight and extensible neuroimaging data processing framework in Python. *Front. Neuroinform* 5, 13 (2011). [PubMed: 21897815]
10. Jenkinson M, Beckmann CF, Behrens TEJ, Woolrich MW & Smith SM FSL. *NeuroImage* 62, 782–790 (2012). [PubMed: 21979382]
11. Esteban O et al. MRIQC: advancing the automatic prediction of image quality in MRI from unseen sites. *PLoS One* 12, e0184661 (2017). [PubMed: 28945803]
12. Gorgolewski KJ et al. The brain imaging data structure, a format for organizing and describing outputs of neuroimaging experiments. *Sci. Data* 3, 160044 (2016). [PubMed: 27326542]
13. Working draft of BIDS Derivatives (BIDS Extension Proposals 3, 11, 12, 13, 14, and 16): representation of the outputs of common processing pipelines. Available at <https://github.com/bids-standard/bids-specification/pull/109> (accessed 18 March 2019) (2019).
14. Ciric R et al. Mitigating head motion artifact in functional connectivity MRI. *Nat. Protoc* 13, 2801–2826 (2018). [PubMed: 30446748]
15. Finc K, Chojnowski M & Bonna K fMRIDenoise: automated denoising, denoising strategies comparison, and functional connectivity data quality control. 10.5281/zenodo.3383310 (accessed 30 September 2019) (2019).
16. Detre JA, Leigh JS, Williams DS & Koretsky AP Perfusion imaging. *Magn. Reson. Med* 23, 37–45 (1992).

17. Qiu D, Zaharchuk G, Christen T, Ni WW & Moseley ME Contrast-enhanced functional blood volume imaging (CE-fBVI): enhanced sensitivity for brain activation in humans using the ultrasmall superparamagnetic iron oxide agent ferumoxytol. *NeuroImage* 62, 1726–1731 (2012). [PubMed: 22584230]
18. Lu H, Golay X, Pekar JJ & van Zijl PCM Functional magnetic resonance imaging based on changes in vascular space occupancy. *Magn. Reson. Med* 50, 263–274 (2003). [PubMed: 12876702]
19. Davis TL, Kwong KK, Weisskoff RM & Rosen BR Calibrated functional MRI: mapping the dynamics of oxidative metabolism. *Proc. Natl Acad. Sci. USA* 95, 1834–1839 (1998). [PubMed: 9465103]
20. Sikka S et al. Towards automated analysis of connectomes: the configurable pipeline for the analysis of connectomes (C-PAC). in 5th INCF Congress of Neuroinformatics. 117 (2014).
21. Van Essen DC et al. The Human Connectome Project: a data acquisition perspective. *NeuroImage* 62, 2222–2231 (2012). [PubMed: 22366334]
22. Glasser MF et al. The minimal preprocessing pipelines for the Human Connectome Project. *NeuroImage* 80, 105–124 (2013). [PubMed: 23668970]
23. Poldrack RA, Mumford JA & Nichols TE *Handbook of Functional MRI Data Analysis* (Cambridge University Press, 2011).
24. Mumford JA & Nichols TE Power calculation for group fMRI studies accounting for arbitrary design and temporal autocorrelation. *NeuroImage* 39, 261–268 (2008). [PubMed: 17919925]
25. Nichols TE & Holmes AP Nonparametric permutation tests for functional neuroimaging: a primer with examples. *Hum. Brain Mapp* 15, 1–25 (2002). [PubMed: 11747097]
26. Halchenko YO et al. Open Brain Consent: make open data sharing a no-brainer for ethics committees. 10.5281/zenodo.1411525 (accessed 18 March 2019) (2018).
27. Cox RW & Hyde JS Software tools for analysis and visualization of fMRI data. *NMR Biomed.* 10, 171–178 (1997). [PubMed: 9430344]
28. Avants BB et al. A reproducible evaluation of ANTs similarity metric performance in brain image registration. *NeuroImage* 54, 2033–2044 (2011). [PubMed: 20851191]
29. Fischl B *FreeSurfer*. *NeuroImage* 62, 774–781 (2012). [PubMed: 22248573]
30. Abraham A et al. Machine learning for neuroimaging with scikit-learn. *Front. Neuroinform* 8, 14 (2014). [PubMed: 24600388]
31. Kennedy DN et al. Everything matters: the ReproNim perspective on reproducible neuroimaging. *Front. Neuroinform* 13, 1 (2019). [PubMed: 30792636]
32. Halchenko YO et al. Open Source Software: Heudiconv. 10.5281/zenodo.1012598 (accessed 18 March 2019) (2018).
33. Yoo AB, Jette MA & Grondona M SLURM: simple Linux utility for resource management in Job Scheduling Strategies for Parallel Processing (eds. Feitelson D, Rudolph L & Schwiegelshohn U) 44–60 (Springer, 2003).
34. Kurtzer GM, Sochat V & Bauer MW Singularity: scientific containers for mobility of compute. *PLoS One* 12, e0177459 (2017). [PubMed: 28494014]
35. Feingold F, Esteban O & Markiewicz C fMRIPrep tutorial: running the docker image. 10.5281/zenodo.2597592 (accessed 18 March 2019) (2019).
36. Esteban O et al. Open Source Software: Task fMRI Analysis using FSL and data preprocessed with fMRIPrep. 10.5281/zenodo.2634481 (accessed 10 April 2019) (2019).
37. Smith SM & Brady JM SUSAN—a new approach to low level image processing. *Int. J. Comput. Vis* 23, 45–78 (1997).
38. Woolrich MW, Ripley BD, Brady M & Smith SM Temporal autocorrelation in univariate linear modeling of FMRI data. *NeuroImage* 14, 1370–1386 (2001). [PubMed: 11707093]
39. Woolrich MW, Behrens TEJ, Beckmann CF, Jenkinson M & Smith SM Multilevel linear modelling for FMRI group analysis using Bayesian inference. *NeuroImage* 21, 1732–1747 (2004). [PubMed: 15050594]

40. Mechelli A, Friston KJ & Price CJ The effects of presentation rate during word and pseudoword reading: a comparison of PET and fMRI. *J. Cogn. Neurosci* 12, 145–156 (2000). [PubMed: 11506654]
41. Mechelli A, Gorno-Tempini ML & Price CJ Neuroimaging studies of word and pseudoword reading: consistencies, inconsistencies, and limitations. *J. Cogn. Neurosci* 15, 260–271 (2003). [PubMed: 12676063]
42. Gorgolewski KJ et al. BIDS apps: improving ease of use, accessibility, and reproducibility of neuroimaging data analysis methods. *PLoS Comput. Biol* 13, e1005209 (2017). [PubMed: 28278228]
43. Tustison NJ et al. N4ITK: improved N3 bias correction. *IEEE Trans. Med. Imaging* 29, 1310–1320 (2010). [PubMed: 20378467]
44. Dale AM, Fischl B & Sereno MI Cortical surface-based analysis: I. segmentation and surface reconstruction. *NeuroImage* 9, 179–194 (1999). [PubMed: 9931268]
45. Klein A et al. Mindboggling morphometry of human brains. *PLoS Comput. Biol* 13, e1005350 (2017). [PubMed: 28231282]
46. Fonov V et al. Unbiased average age-appropriate atlases for pediatric studies. *NeuroImage* 54, 313–327 (2011). [PubMed: 20656036]
47. Avants BB, Epstein CL, Grossman M & Gee JC Symmetric diffeomorphic image registration with cross-correlation: evaluating automated labeling of elderly and neurodegenerative brain. *Med. Image Anal* 12, 26–41 (2008). [PubMed: 17659998]
48. Zhang Y, Brady M & Smith S Segmentation of brain MR images through a hidden Markov random field model and the expectation-maximization algorithm. *IEEE Trans. Med. Imaging* 20, 45–57 (2001). [PubMed: 11293691]
49. Huntenburg JM Evaluating nonlinear coregistration of BOLD EPI and T1w images (Freie Universität, Berlin, Germany, 2014).
50. Wang S et al. Evaluation of field map and nonlinear registration methods for correction of susceptibility artifacts in diffusion MRI. *Front. Neuroinform* 11, 17 (2017). [PubMed: 28270762]
51. Treiber JM et al. Characterization and correction of geometric distortions in 814 diffusion weighted images. *PLoS One* 11, e0152472 (2016). [PubMed: 27027775]
52. Greve DN & Fischl B Accurate and robust brain image alignment using boundary-based registration. *NeuroImage* 48, 63–72 (2009). [PubMed: 19573611]
53. Jenkinson M, Bannister P, Brady M & Smith S Improved optimization for the robust and accurate linear registration and motion correction of brain images. *NeuroImage* 17, 825–841 (2002). [PubMed: 12377157]
54. Power JD et al. Methods to detect, characterize, and remove motion artifact in resting state fMRI. *NeuroImage* 84, 320–341 (2014). [PubMed: 23994314]
55. Behzadi Y, Restom K, Liao J & Liu TT A component based noise correction method (CompCor) for BOLD and perfusion based fMRI. *NeuroImage* 37, 90–101 (2007). [PubMed: 17560126]
56. Lanczos C Evaluation of noisy data. *J. Soc. Ind. Appl. Math. Ser. B Numer. Anal* 1, 76–85 (1964).

Box 1 |**BIDS**

BIDS¹² is a standard for organizing and describing brain datasets, including MRI. The common naming convention and folder structure allow researchers to easily reuse BIDS datasets, reapply analysis protocols and run standardized automatic data preprocessing pipelines such as fMRIPrep. The BIDS starter kit (<https://github.com/bids-standard/bids-starter-kit>) contains a wide collection of educational resources.

Validity of the structure can be assessed with the BIDS Validator (<https://bids-standard.github.io/bids-validator/>). The tree of a typical, valid (BIDS-compliant) dataset is shown. Further instructions and documentation on BIDS are found at <https://bids.neuroimaging.io>. In this protocol, we use OpenNeuro's ds000003⁸ as the base dataset.

```
ds000003/
├── CHANGES
├── dataset_description.json
├── participants.tsv
├── README
├── sub-01/
│   ├── anat/
│   │   ├── sub-01_inplaneT2.nii.gz
│   │   └── sub-01_T1w.nii.gz
│   └── func/
│       ├── sub-01_task-rhymejudgment_bold.nii.gz
│       └── sub-01_task-rhymejudgment_events.tsv
├── sub-02/
└── sub-03/
```

Box 2 |**Using DataLad to fetch a BIDS dataset from OpenNeuro**

DataLad (<https://www.datalad.org>) is a convenient scientific data management tool that allows access to all data hosted in OpenNeuro. First, visit the OpenNeuroDatasets organization at GitHub (<https://github.com/OpenNeuroDatasets>) and locate the dataset by its accession identifier (in this example, ds000003). Then, visit the repository of the dataset and copy the URL provided by the ‘Clone or download’ green button (top right), placing it as the argument to the datalad install tool as follows: `dataladinstall-https://github.com/OpenNeuroDatasets/ds000003.git`

For directions on the installation of DataLad, please follow the instructions given in its documentation.

Box 3 |**BIDS-Derivatives data structure**

The directory tree of a BIDS-Derivatives¹³ dataset generated from a run of fMRIPrep is shown below:

```
derivatives/
├── fmriprep/
│   ├── dataset_description.json
│   ├── logs
│   ├── sub-01.html
│   └── sub-01/
│       ├── anat/
│       │   ├── sub-01_desc-brain_mask.nii.gz
│       │   ├── sub-01_dseg.nii.gz
│       │   ├── sub-01_label-GM_probseg.nii.gz
│       │   ├── sub-01_label-WM_probseg.nii.gz
│       │   ├── sub-01_label-CSF_probseg.nii.gz
│       │   ├── sub-01_desc-preproc_T1w.nii.gz
│       │   ├── sub-01_space-MNI152_desc-brain_mask.nii.gz
│       │   ├── sub-01_space-MNI152_dseg.nii.gz
│       │   ├── sub-01_space-MNI152_label-GM_probseg.nii.gz
│       │   ├── sub-01_space-MNI152_label-WM_probseg.nii.gz
│       │   ├── sub-01_space-MNI152_label-CSF_probseg.nii.gz
│       │   ├── sub-01_space-MNI152_desc-preproc_T1w.nii.gz
│       │   ├── sub-01_from-MNI152_to-T1w_mode-image_xfm.h5
│       │   ├── sub-01_from-T1w_to-MNI152_mode-image_xfm.h5
│       │   └── sub-01_from-orig_to-T1w_mode-image_xfm.txt
│       ├── figures/
│       └── func/
│           ├── sub-01_task-rhymejudgment_space-MNI152_boldref.nii.gz
│           ├── sub-01_task-rhymejudgment_space-MNI152_desc-preproc_bold.nii.
│           ├── sub-01_task-rhymejudgment_space-MNI152_desc-confounds_regress
│           └── sub-01_task-rhymejudgment_space-MNI152_desc-brain_mask.nii.gz
├── sub-02.html
├── sub-02/
├── sub-03.html
└── sub-03/
```

Box 4 |**Citation boilerplate**

The visual reports generated for every subject contain an excerpt that can be copied and pasted directly into papers using fMRIPrep, to ensure that preprocessing of data is reported transparently:

Results included in this manuscript come from preprocessing performed using fMRIPrep⁷ 1.4.1 (RRID:SCR_016216), which is based on Nipype⁹ 1.1.6 (RRID:SCR_002502). An exemplar analysis workflow with FSL¹⁰ tools was carried out. First level analysis utilizes FILM³⁸ (FMRIB's Improved Linear Model) to set up a standard generalized linear model (GLM). Based on the outcomes of first level analysis, group level inference is conducted with FLAME³⁹ (FMRIB's Local Analysis of Mixed Effects).

Anatomical data preprocessing.

The T1w image was corrected for intensity non-uniformity with N4BiasFieldCorrection⁴³ (ANTs 2.2.0, RRID: SCR_004757) and used as a T1w-reference throughout the workflow. The T1w-reference was then skull-stripped with antsBrainExtraction.sh (ANTs 2.2.0) using OASIS (Open Access Series of Imaging Studies) as a target template. Brain surfaces were reconstructed with recon-all⁴⁴ (FreeSurfer 6.0.1, RRID: SCR_001847), and the brain mask estimated previously was refined with a custom variation of the method to reconcile ANTs-derived and FreeSurfer-derived segmentations of the cortical gray matter (GM) of Mindboggle⁴⁵ (RRID: SCR_002438). Spatial normalization to the ICBM 152 Nonlinear Asymmetrical template⁴⁶ version 2009c ('MNI152NLin2009cAsym'; RRID: SCR_008796) was performed through nonlinear registration with antsRegistration⁴⁷ (ANTs 2.2.0), using brain-extracted versions of both T1w volume and template. Brain tissue segmentation of cerebrospinal fluid (CSF), white matter (WM) and GM was performed on the brain-extracted T1w with FAST⁴⁸ (FSL 5.0.9, RRID: SCR_002823).

Functional data preprocessing.

For each of the BOLD runs found per subject (across all tasks and sessions), the following preprocessing was performed. First, a reference volume and its skull-stripped version were generated with a custom methodology of fMRIPrep (described within the documentation of the tool, <https://fmripred.org>). A deformation field to correct for susceptibility distortions was estimated based on fMRIPrep's fieldmap-less approach. The deformation field results from co-registering the BOLD reference to the same-subject T1w reference with its intensity inverted^{49,50}. Registration is performed with antsRegistration (ANTs 2.2.0), and the process is regularized by constraining deformation to be nonzero only along the phase-encoding direction, and modulated with an average fieldmap template⁵¹. Based on the estimated susceptibility distortion, an unwarped BOLD reference was calculated for more accurate co-registration with the anatomical reference. The BOLD reference was then co-registered (six degrees of freedom) to the T1w reference with bregister (FreeSurfer), which implements boundary-

based registration⁵². Head-motion parameters with respect to the BOLD reference (transformation matrices and six corresponding rotation and translation parameters) were estimated before any spatiotemporal filtering with MCFLIRT⁵³ (Motion-Correction FMRIB's Linear Image Registration Tool, FSL 5.0.9). The BOLD time-series were resampled onto their original, native space by applying a single, composite transform to correct for head-motion and susceptibility distortions. These resampled BOLD time-series will be referred to as preprocessed BOLD in original space, or just preprocessed BOLD. The BOLD time-series were resampled to MNI152NLin2009cAsym standard space, generating a preprocessed, spatially normalized BOLD run. Several confounding time-series were calculated based on the preprocessed BOLD: framewise displacement, DVARS and three region-wise global signals. Frame displacement and DVARS were calculated for each functional run, both using their implementations in Nipype (following the definitions by Power et al.⁵⁴). The three global signals were extracted within the CSF, the WM and the whole-brain masks. In addition, a set of physiological regressors were extracted to allow for CompCor⁵⁵. Principal components were estimated after high-pass filtering the preprocessed BOLD time-series (using a discrete cosine filter with a 128-s cut-off) for the two CompCor variants: temporal and anatomical. Six temporal CompCor components were then calculated from the top 5% variable voxels within a mask covering the subcortical regions. This subcortical mask was obtained by heavily eroding the brain mask, which ensured that it did not include cortical GM regions. For anatomical CompCor, six components were calculated within the intersection of the aforementioned mask and the union of CSF and WM masks calculated in T1w space, after their projection to the native space of each functional run (using the inverse BOLD-to-T1w transformation). The head-motion estimates calculated in the correction step were also placed within the corresponding confounds file. All resamplings were performed with a single interpolation step by composing all the pertinent transformations (i.e., head-motion transform matrices, susceptibility distortion correction when available and co-registrations to anatomical and template spaces). Gridded (volumetric) resamplings were performed with ANTs, configured with Lanczos interpolation to minimize the smoothing effects of other kernels⁵⁶. Non-gridded (surface) resamplings were performed with `mri_vol2surf` (FreeSurfer).

Many internal operations of fMRIPrep use Nilearn³⁰ 0.5.0 (RRID: SCR_001362), mostly within the functional processing workflow. For more details on the pipeline, see the section corresponding to workflows in fMRIPrep's documentation (<https://fmripred.org>).

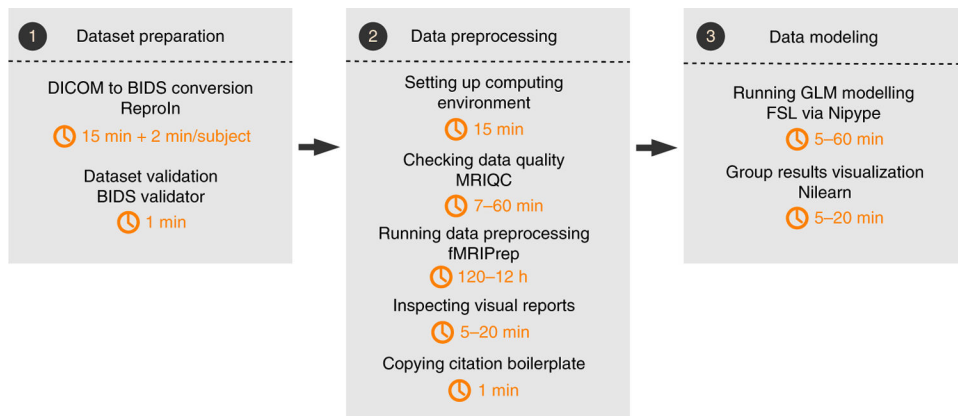


Fig. 1 | Overall workflow of the fMRIPrep protocol.

The analytic workflow is subdivided into three principal stages. First, a BIDS-compliant dataset is generated and validated. Next, dataset quality is assessed, and the data are preprocessed. Finally, the preprocessed data undergo a GLM fitting, which yields participant- and group-level statistical maps of task-related BOLD activity. FSL, FMRIB Software Library.

```

#!/bin/bash
#
#SBATCH -J fmriprep
#SBATCH --array=1-13
#SBATCH --time=16:00:00
#SBATCH -n 1
#SBATCH --cpus-per-task=16
#SBATCH --mem-per-cpu=4G
#SBATCH -p russpold,owners,normal
# Outputs -----
#SBATCH -o log/%x-%A-%a.out
#SBATCH -e log/%x-%A-%a.err
#SBATCH --mail-user=%u@stanford.edu
#SBATCH --mail-type=ALL
# -----

unset PYTHONPATH
export SINGULARITYENV_FS_LICENSE=$STUDY/.freesurfer.txt
export SINGULARITYENV_TEMPLATEFLOW_HOME=$STUDY/.templateflow

BIDS_DIR="$STUDY/ds000003"
OUTPUT_DIR="${BIDS_DIR}/derivatives/fmriprep-1.4.1"

SINGULARITY_CMD="singularity run -e $STUDY/fmriprep-1.4.1.simg"

subject=$( sed -n -E \
"$({SLURM_ARRAY_TASK_ID} + 1) s/sub-(\S*)\>.*\|1/gp" \
${BIDS_DIR}/participants.tsv )

cmd="${SINGULARITY_CMD} ${BIDS_DIR} ${OUTPUT_DIR} participant \
--participant-label $subject \
-w $L_SCRATCH/work/ \
--omp-nthreads 8 --nthreads 12 --mem_mb 30000 \
--output-spaces MNI152NLin2009cAsym:res-2 anat \
--use-syn-sdc"

echo Running task ${SLURM_ARRAY_TASK_ID}
echo Commandline: $cmd
eval $cmd
exitcode=$?
echo "sub-$subject ${SLURM_ARRAY_TASK_ID} $exitcode" \
>> ${SLURM_ARRAY_JOB_ID}.tsv
echo Finished tasks ${SLURM_ARRAY_TASK_ID} with exit code $exitcode
exit $exitcode

```

Scheduler settings

We define a new job called 'fmriprep', which will parallelize tasks with indexes 1–13, with a wall-clock time of 16 h (please allocate ≥ 12 h for FreeSurfer to run completely).

Each task will be run in just one node ('-n 1'), will use 16 CPUs on that node, and 64 GB of RAM will be requested to the node. In our settings, we could submit to three allocations called 'russpold', 'owners' and 'normal' of Stanford's Sherlock Cluster.

Some additional tracing options are set at the bottom of this preamble.

Controlling the environment: make sure the PYTHONPATH does not traverse into the container, and set an existing FS license file (via SINGULARITYENV_* magic variables).

Defining input/output paths

Singularity run command and image

Select one subject from the participants.tsv file, which is to be run within this task of the job-array.

BIDS apps interface: both fMRIPrep and MRIQC have a uniform interface:

```
app_executable input/ output/ <level>
<arguments>
```

The remainder of the file executes the command line and keeps track of the exit status of each task for troubleshooting purposes.

Fig. 2 |. Running fMRIPrep on HPC.

Execution of BIDS apps⁴² (such as MRIQC or fMRIPrep) is easy to configure on HPC clusters. This figure provides an example execution script for our SLURM-based cluster, Stanford's Sherlock. An up-to-date, complete version of the script is available at <https://fmriprep.readthedocs.io/en/latest/singularity.html#running-singularity-on-a-slurm-system>.

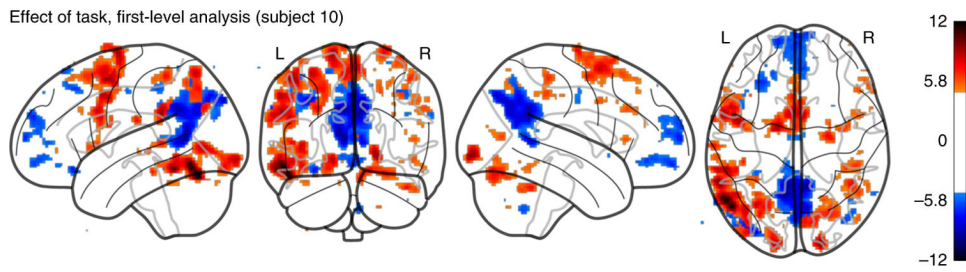


Fig. 3 |. Output of the first-level analysis step.

Glass brain visualization of a statistical (z -stat) map reflecting the ‘intask-vs.-nontask’ activation obtained for subject 10 (thresholded at $z = \pm 5$).

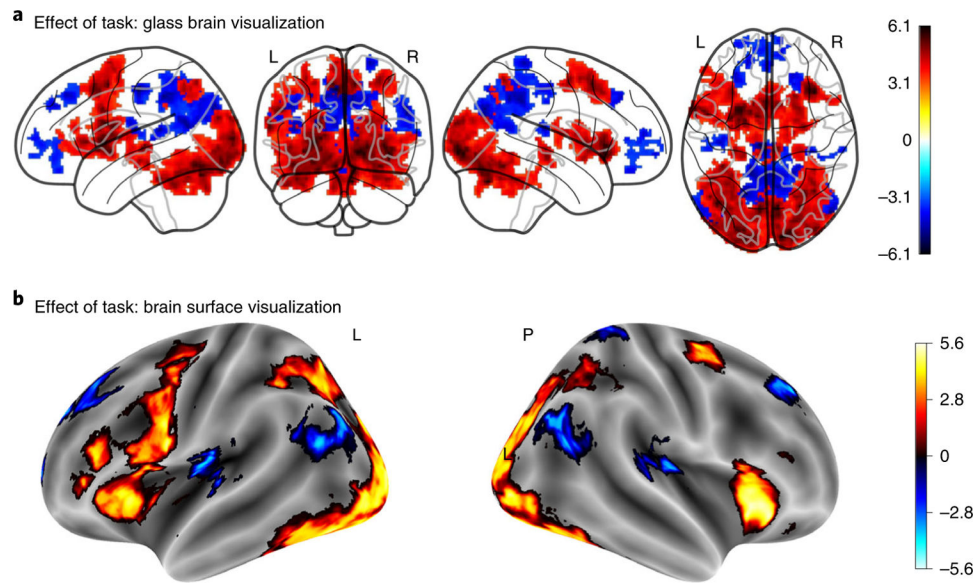


Fig. 4 |. Group analysis results.

Visualization of a group statistical (z -stat) map (cluster threshold = 3.2) reflecting the ‘task-vs.-nontask’ activation for all subjects. **a**, Glass brain visualization. **b**, Left and right hemisphere surface plot visualizations. Visualizations were generated using a function from Nilearn (see Visualization of results for details).

Table 1 |

Comparison of fMRI preprocessing workflows

	fMRIPrep	AFNI afni_proc.py	C-PAC	HCP pipelines	FSL FEAT
Scope	Preprocessing	End to end ^a	End to end	End to end	End to end
Acquisition protocol	Any (self-adaptive)	Any (configurable)	fMRI (configurable)	HCP-like protocols	Any (configurable)
BIDS	Required	In progress	Supported	Unsupported	Unsupported
BIDS-Derivatives	Compliant	In progress	In progress	Unsupported	Unsupported
Single-subject, single-run	Auto	Auto	Auto	Auto	Auto
Single-subject, multi-run	Auto	Manual	Auto	Auto	Manual
Multi-subject	Auto	Manual	Auto	Manual	Manual
Source license	Open (BSD)	Open (GPL)	Open (BSD)	Open (BSD)	Open (Custom)
Use restrictions	Non-commercial ^b	None	Non-commercial ^b	Non-commercial ^b	Non-commercial
Community-driven	Yes	No	No	No	No
Combines packages	Yes	No	Yes	Yes	No
Open CI/CD	Yes	No	No	No	No
Containerization	Full	Full	Full	Third party	Third party
BIDS-App	Full	In progress	Full	Third-party	N/A
User interface	CLI	GUI, CLI	SFI ^c	CLI	SFI
Manual operation	Minimal	Extensive	Minimal ^d	Limited	Extensive
Self-documenting ^e	Yes	No	No	No	No
Output spaces	Vol., surf., mixed	Volume ^f	Volume	Mixed	Volume
TemplateFlow	Yes	N/A	N/A	N/A	N/A
CIFTI2 grayordinates	Full (v20+)	N/A	N/A	Full	N/A

We excluded statistical parametric mapping (SPM) from the comparison since it does not support automatic processing without the use of extensions. AFNI, analysis of functional neuroimages; BDS, Berkeley Software Distribution; CI/CD, continuous integration and delivery; CLI, command-line interface; C-PAC, Configurable Pipeline for the Analysis of Connectomes; FEAT, FMRI Expert Analysis Tool; GPL, GNU Public License; GUI, graphical user interface; N/A, not available; SFI, settings file interface; surf., surface-space; Vol., volume-space.

^aAlthough these tools do not prescribe specific tailored analysis, the user is required to adapt the outputs to new tools other than the one used to generate the preprocessed inputs in the first place.

^bDue to the use of FSL, which has noncommercial restrictions.

^cThe user prescribes the processing steps via a configuration file, which can be generated with a GUI helper.

^dManual operation is not necessary when using default settings; for more sophisticated configurations, pervasive manual operation is required.

^e'Self-documenting' refers to the possibility of dynamically generating a description in natural language containing all the details about the executed processing workflow, including references to the scientific literature.

^fSurface analysis is possible with AFNI SUrface MApper.